Design and Development of a Humanoid with Articulated Torso

Divyanshu Goel[1], S Phani Teja[1], Parijat Dewangan[1], Suril V Shah[2], Abhishek Sarkar[1], K Madhava Krishna[1]

***Abstract*— The purpose of this paper is to present the model of a Humanoid robot inspired by Poppy, modified for heavier load capacity and the balancing of humanoid in multiple work environments. The design has been modified in order to use MX-64 servos with more torque capacity than MX-28 servos which were used in original design. We have also redesigned the ankle joint and feet to make it a more accurate human like model. We are using an integrated approach using zero moment point (ZMP) with force sensing resistor (FSR) and center of mass (CoM) to find balance margins of the robot. Balancing and forward bending experiments on robot are conducted by providing some basic motion to the robot and ensuring that the robot is balanced and moving within safe margins using this approach.**

I. Introduction

Humanoids can be employed in many areas of industry, defense, construction, health care, agriculture and many other places where a complex manipulator with versatile locomotion is needed. Humanoid robots have been the topic of much research in order to replicate the similar motion as seen in humans so as to achieve same degree of flexibility and agility as human beings [1], [2]. It has the supreme characteristics to work as human substitutes, as they can perform well in human environments and assist people in daily life, considering most of the machines are designed for human operation and this allows for robots to work directly in such environments. However, the dynamics involved with the humanoid is complex, non-linear and difficult to control [3]. Researchers all over the world have tried various different approaches for controlling the dynamics of the bipeds [3]. Many methods, including offline trajectory control, feedback system involving different sensors [3] have been developed. Also, such platform costs a lot of time and money to build and thus were not publicly available. But, recently advances in rapid prototyping have drastically solved the availability problem, a few of such robots are listed in Table no. I.

ZMP as defined by Vukobratovic [4] is one of the important criteria while considering the dynamic stability of any biped. In order to be dynamically stable, ground projection of CoM should lie within the convex hull of the feet of humanoid, which is also known as the support polygon of the system. One of the important feedback mechanism is using the data of the ground reaction force to track the Center of Pressure (CoP) of the system and hence dynamically control the stability of the humanoid. ZMP helps us in achieving dynamically stable gait, for instance, in case of picking up of a heavy object and perform other day to day tasks. We need to analyze the inertia of the object in order to adjust the joint angles and torques. Position of ZMP is a crucial criteria in adjusting the joint angles (mainly, knee and abdominal) in the above complex situation for maintaining balance. It's required to limit the motion of the humanoid accordingly even if the physical joint limits due to the mechanical constraints allow certain static configuration, to prevent it from falling by using the ZMP criteria.

Despite being a practical criteria, actions like jumping and running are not dynamically stable according to this criteria. Biological feedback of human-like walking is also not dynamically stable according to ZMP criteria [5].

As technology is advancing, precise and multi-directional force and torque sensors can be used to obtain ZMP information, for instance, 6 Degree of freedom (DOF) force and torque sensor made by Nitta Corp that is used in HRP-2 [6]. Our choice of force sensors also depends on various other factors. We used FSR built by TekScan [7] which can measure up to 11.3 Kg for the foot, keeping in mind its low cost, lightness, thinness and compatibility with the designed foot. FSR varies its resistance depending upon how much force is applied on its sensing area. Using multiple FSRs yields reliable results in the determination of ZMP.

TABLE I: Comparison of different humanoids

Name	Mass (Kg)	Height (cm)	DOF	Spine DOF
iCub [8]	23	100	53	3
DarwinOP [9]	2.9	45.4	20	0
Nao[10]	5.4	87.4	24	0
Poppy [11]	3.5	83	25	5
Wabian [12]	64	150	41	2
Kenta [13]	19	123	80	30
Robota[14]	1.5	45	9	0

Our main focus is on deploying the humanoid in Urban Search and Rescue (USAR) operations. The recent DARPA challenge shows the deployment of humanoids/bipeds in such scenarios. None of these robots took the help of surrounding environment to increase support polygon area [15]. Our aim is to make the humanoid design more robust so that it can use the surrounding environment in the USAR

[1] Divyanshu Goel, S Phani Teja, Parijat Dewangan, Abhishek Sarkar and K Madhava Krishna are with the Robotics Research Lab, IIIT-Hyderabad, TS 500032, India. {divyanshu.goel, singamaneniphani.teja, parijat.dewangan}@research.iiit.ac.in, {abhishek.sarkar, mkrishna}@iiit.ac.in

[2] Suril V Shah is with Department of Mechanical Engineering, IIT Jodhpur, Rajasthan 342011, India. surilshah@iitj.ac.in

978-1-5090-5203-5/16/ $31.00 ©2016 IEEE

situations and be stable while it is traversing in such terrains.

In this paper, the design and development of a humanoid robot is discussed with advantages and disadvantages. We have done simulations and experiments to find the stability margins for our robot and discussed design of basic sensor feedback systems. Using the provided systems, we have conducted simple experiments to explain its importance in maintaining stability, which is the basic necessity in humanoid robots.

The paper is organized as follows. In Section II, the model of the robot is explained underlining the modifications in design and structure. Sensor placement and ZMP details are explained in Section III along with the equations required for ZMP calculation. The simulation results of the humanoid balancing and change in CoM is shown and analyzed in Section IV. Section V shows the experimental results on the real humanoid robot. Finally, conclusions and future work are discussed in Section VI.

II. MODEL OF ROBOT

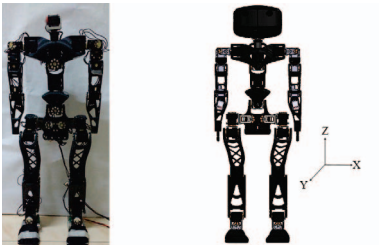

Fig. 1: 3D printed Humanoid (left) and CAD model (right)

A. Mechanical Design

To be able to exploit the surrounding environment in a USAR setting, the robot design has to be robust enough to traverse such terrains. For this reason the robot is made light weight i.e. less than 5 Kg. Also, all the parts are 3D printed which makes the replacement of the parts easier and allows building the prototype quickly. The structural design as shown in Fig. 1, is a modified form of the robot used in the Poppy project [11]. We want to make it a self contained robot with the capacity to avoid falls and stand back up. However, before we achieve that, making the robot stable is an integral part. As a step towards this, the most desirable feature in a humanoid is a flexible vertebral column [16]. The robot has 27 DOF (presented in Section C). The height is approximately 84 cm which is roughly half of the average human height. Also, it's height is more than most of the other similar robotic platforms like NAO (57.4 cm) [10], DarwinOP (45.45 cm) [9] as shown in Table No. I. The entire robot is 3D printed with PLA material which has density 1250 $\mathrm{kg/m^3}$, breaking tensile strength is 48.8 MPa and thus it is sturdy without adding up too much weight to the total structure keeping it lightweight.

B. Architecture

1. Humanoid :- The humanoid body is divided into different sections - legs, hands, torso and head. The overall platform is small, with total height 84 cm, total weight under 5 Kg and 27 DOF. Shoulder has 2 motors emulating universal joints and elbow too has a similar setup of universal joint. The lower body can be considered as a single entity, without upper body, allowing us to simplify the planning for locomotion. Thus, we can see the robot in two halves maintaining CoM of each separately and easily.

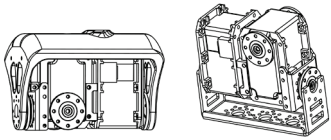

Fig. 2: Universal joint at (a) abdomen (b) ankle

2. Upper Body :- The torso has 5 joints emulating a simpler vertebral column. As designed in Poppy, the vertebral column can be viewed as a joining link between shoulders and pelvis having two universal joints, containing two revolute joints as shown in Fig. 2(a) and a single revolute joint in the middle. These 5 joints allow us to free the lower body from the constraints of the upper body and adjust the CoM without solely relying on the pelvic joint. Additionally this design also increases the effective work space of the entire arm assembly and brings it one step closer to achieve universal reach within the work-space in order to pick and place objects.

3. Lower Body :-The leg section emulates a spherical joint at the hip by using 3 servo motors, a single revolute joint at the knee and emulating a universal joint at ankle allowing for sagittal and frontal motion. Since there is no universal joint in the ankle of Poppy it is difficult to adapt to uneven terrain. So we added an extra DOF at both the ankles as shown in Fig. 2(b).

C. Changes from the design of Poppy

The problem with Poppy robot was that the motor output torque was low and as a result the robot was unable to stand properly if the links were changed or made heavier. However, as done in Poppy we are using servo motors but in order to increase the capacity of the robot, various motors of Poppy are replaced with the higher torque variety model. The motors used in the modified humanoid are Dynamixel MX-64 (6 N-m torque) instead of Dynamixel MX-28 (2.5 N-m torque) model. The motor has contact-less magnetic

sensor of 0.1° resolution and can give feedback of angular velocity and angular acceleration directly. It also has in-built PID controller and the global feedback loop gives us angular position, velocity and acceleration of motors. Therefore, compliance of the motor joints can be simulated by changing the PID values [17].

The above discussed change also constitutes changes in geometry and design of the whole body to make space for these motors and make the links stronger for higher load carrying capacity, while still retaining the necessary bend in the legs [11], which allows closer placement of CoM in the support polygon for greater stability. The foot thickness was very small in the original Poppy design. We have redesigned the foot as a firm sole. We also have separated the toe and introduced a torsion spring to allow for elastic property in foot. We introduced an extra DOF at ankles allowing motion in frontal plane as well, which was not originally present in Poppy thus allowing to tilt the robot sideways.

The arms were also modified in order to have an actuated hand controlled by a single motor in each hand to grasp small objects. The backlash problem in servo at ankle and knee joints in humanoid in Poppy is solved by using springs but we have not used them as its negligible for small links. The flexibility of our structure allows us to do more complex tasks in complex environments than a normal USAR robot which has limited operations, as it allows the robot to adapt to the environment. In comparison to other similar robots, the presented design is simple, lightweight, and easily modifiable allowing change of links, in case we need to update them.

D. Electronics Specification

The humanoid is powered by a 14.4 V regulator and is controlled in Robotics Operating System (ROS) framework installed in Ubuntu on a PC . The communication happens via USB using a USB -TTL FTDI serial connector. The Dynamixel library (Python) executed in ROS Indigo controls all the motors which are connected in a daisy chain and can communicate using serial protocol. The inertial motion sensing unit (IMU) is placed at the bottom pelvic joint location and gives filtered yaw pitch roll data at 50 Hz frequency.

E. Controller

The basic outline and flow diagram of the motor controller is shown in Fig. 3. The desired angle input to motors is

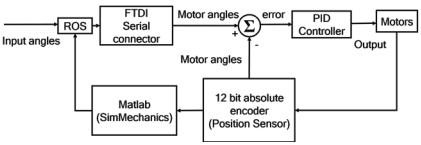

Fig. 3: Block Diagram of motor controller

governed by ROS and fed to the robot through a serial connector. This is read through MATLAB to get details for calculation of CoM coordinates and hence adjust input to the motor accordingly through ROS.

III. ZMP CALCULATIONS AND SENSORS PLACEMENT

The distribution of ground reaction forces on the foot is complicated (Fig. 4(a)) and can't be measured accurately. So, CoP [4] is used to tackle this issue. It is one of the crucial factors for controlling the dynamic balance of the biped.

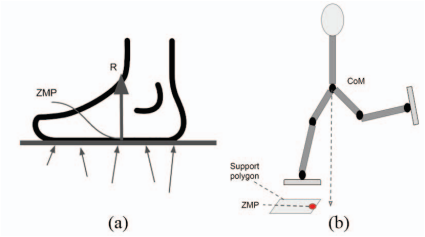

Fig. 4: (a) Ground reaction force and ZMP (b) Relation between CoM and ZMP

The ZMP always lies inside the support polygon (convex hull of the feet) [18]. During static stability, the ground projection of CoM and ZMP coexist and lie within the support polygon. On the contrary, for dynamic balance the ground projection of CoM may lie outside the support polygon. Fig. 4(b) illustrates the relationship between the ZMP, CoM and the support polygon in case of instability [18]. If the projection of CoM on the ground lies outside support polygon, then ZMP lies at the edge of support polygon. We can use these two criteria for various applications like fall detection and balancing of biped. Thus, ZMP coupled with ground projection of CoM can be used as one of the factors for determining the stability margin of the robot.

A. ZMP calculation and FSR placement

We have used four low cost 1-D FSRs in each foot, two in the front and two in the back for calculation of CoP as shown in Fig. 5. They are used to measure the ground reaction force only in the vertical direction. For evaluation of ZMP, we have used normalized data, only in vertical direction.

When the robot is standing still on a horizontal ground plane, constant contact forces are applied on the FSRs. But as any joint motor is actuated, the contact force of the foot changes and hence the FSR values also change. For any foot, when the robot lifts the heel while its toes still touching the ground, the sensors 1 and 2 will give high readings where as the readings from 3 and 4 are negligible. Thus, we can detect the tilting of the robot in any direction by properly analyzing the FSR readings.

CoP is calculated after calibrating all the FSRs with respect to origin O as shown in Fig. 5, where origin O is

at the projection of CoM of humanoid when all the motors are at zero degrees. We take benefit of the fact that CoP and ZMP coincides [19], [18]. The CoP/ZMP can be calculated by following equation :

$$p_x = \frac{\sum_{i=1}^{N=4} p_{ix} f_{iz}}{\sum_{i=1}^{N=4} f_{iz}}$$
$$p_y = \frac{\sum_{i=1}^{N=4} p_{iy} f_{iz}}{\sum_{i=1}^{N=4} f_{iz}} \quad (1)$$

where p_{ix} and p_{iy} refer to position of the ith FSR along x and y direction respectively and f_{iz} refer to the vertical force (z-direction) measured by the ith FSR. The above equation yields CoP coordinates for individual foot. We need to average respective values of each foot to get CoP coordinates in double support phase.

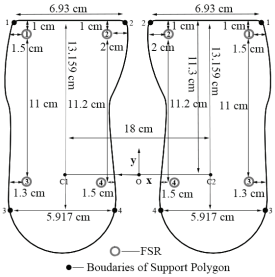

Fig. 5: FSR placement with respect to the origin

IV. SIMULATION RESULTS

Forward bending task was chosen as it plays a major role in shifting the COM in forward direction which is an essential factor for walking [20]. Robot starts from a stable posture with the ground projection of CoM inside the support polygon. Simulations were carried out for motor controlling the pitch of abdomen as shown in Fig. 6, simultaneously controlling pitch motion of right arm by raising it to 90° and measuring the resulting CoM. The ground projection of CoM is same as ZMP in the static stability as explained in the previous section.

The forward bending task is simulated by providing cycloidal trajectory as given in Eq. 2 to abdomen and shoulder motors.

$$P(t) = P_0 + (\frac{t}{t_f} - \frac{1}{2\pi}\sin\frac{2\pi t}{t_f})(P_f - P_0) \quad (2)$$

where t_f is the travel time, P_0 is the initial position, *P(t)* is position at time t, P_f is the desired position. The value of t_f for simulation is 0.8 sec.

The simulation is carried out for 3 different cases with abdomen pitch angles 27.5°, 33.23° and 56°. The plots of the CoM in X, Y and Z directions and angular trajectories of shoulder and abdominal joints for three different cases are shown Figs. 7 and 8.

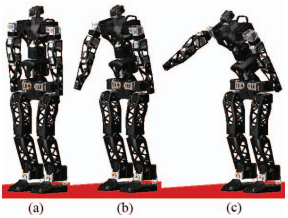

Fig. 6: CAD model of the (a) Robot in initial state (b) Robot bending forward (c) Robot standing stable at the end of abdominal and shoulder bend (case 1)

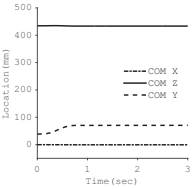

(a) CoM for 27.5°

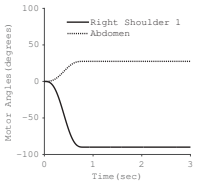

(b) Motor data for 27.5°

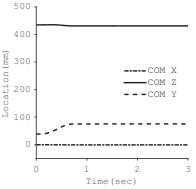

(c) CoM for 33.23°

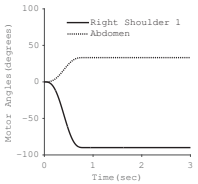

(d) Motor data for 33.23°

Fig. 7: Simulation results for 27.5° and 33.23° forward bend (Stable)

The foot area inside the boundaries of support polygon is defined by the four points on each foot as shown in Fig 5. The coordinates of extremities of the foot are as given in Tables II and III.

The size of support polygon for each foot is 69.3 mm x 131.54 mm. In double support phase, for dynamic stability, ZMP has to lie between (-105.42 mm , 103.29 mm) in X direction and (-19.33 mm , 112.93 mm) in Y direction.

The graphs shown in Fig. 7(a) (case 1: 27.5°) and in Fig. 7(c) (case 2: 33.23°) show that there is motion of CoM in Y direction as the robot is moving only in Y direction. In both of these cases, the projection of CoM falls within the limits of the support polygon. Hence, these two cases can

TABLE II: Left foot

Point	X(mm)	Y(mm)
1	103.29	112.93
2	34.472	112.93
3	103.29	-18.60
4	44.472	-18.60

TABLE III: Right foot

Point	X(mm)	Y(mm)
1	-105.42	112.93
2	-36.11	112.93
3	-105.42	-18.60
4	-46.7	-18.60

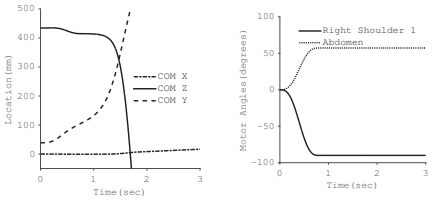

(a) CoM (b) Motor data

Fig. 8: Simulation results for 56° forward bend (Unstable)

be considered as stable. The motor manipulation data for abdomen and shoulder angles for these two cases are shown in Fig. 7(b) and Fig. 7(d).

On the contrary in case 3 (56°), the motion of CoM in Y direction goes on increasing, where as in Z direction it goes on decreasing, implying that the robot is falling. Therefore, this state is considered as unstable (Fig. 8(a)). Fig. 8(b) shows the motor manipulation data provided for this case. This case is the margin of stability in the simulations.

V. EXPERIMENTAL RESULTS

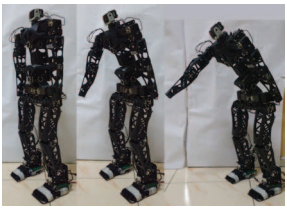

Fig. 9: Experimental image of the (a) Robot in initial state (b) Robot bending forward (c) Robot standing stable at the end of abdominal and shoulder bend (case 1)

Experiments were conducted on the humanoid robot and results have been analyzed for the stable cases found from the simulation. Also experiments were conducted to find the margin of stability while bending forward. For carrying out the experiments cycloidal trajectories for motor manipulation are given as input. FSRs were used to collect real time force feedback (in vertical direction) from the robot. A Razor IMU [21] is placed at the center of the pelvic link, which transmits the data related to yaw, pitch and roll angles of the pelvic link of the robot. The ZMP/CoP is then calculated in real time using Eq. 1. The limits of the ZMP is -111.89 mm to 111.89 mm in X direction and -9 mm to 103 mm in Y direction with respect to origin O in Fig. 5.

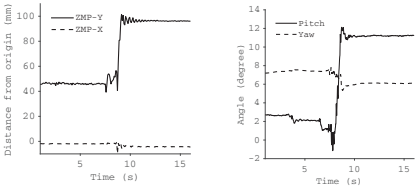

(a) ZMP for 27.5° (b) Pitch and Yaw for 27.5°

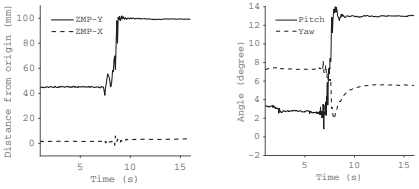

(c) ZMP for 33.23° (d) Pitch and Yaw for 33.23°

Fig. 10: Experimental results for 27.5°, 33.23° forward bend

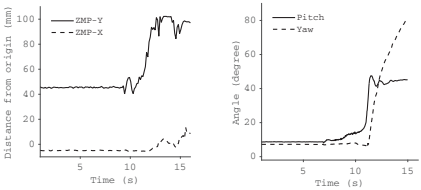

(a) ZMP (b) Pitch and yaw

Fig. 11: Experimental results for 41.82° forward bend

In all these experiments, the robot starts from a stable standing posture and then bends forward with different abdominal and shoulder angles as shown in Fig. 9. The plots of ZMP with time for case I and case II of abdominal angle are given in Fig. 10(a) and 10(c) respectively. As we can see from the plots in Fig. 10, the robot's initial ZMP does not vary. As the robot starts bending forward, we can observe changes in ZMP plots. In Figs. 10(a) and 10(c), ZMP settles down at a value below 100 mm in Y direction which is well within the limits of support polygon making it fully stable.

It was not possible to maintain balance for case III in experiments. So, by trial and error we found the limiting case for stability is 41.82° of abdominal bend where the ZMP value is almost on the edge of the support polygon

(102 mm from origin in Y direction), as shown in Fig. 11. Thus, 41.82° of abdominal angle is the limiting case for stability in forward bend. Further increase in angle resulted in falling of the robot as seen in Fig. 11.

By comparing the Figs. 10(a), 7(a) with 10(c), 7(c) respectively, we observe that the plots of simulation and experiment data are almost similar. The disturbances in experimental data is due to noise, hardware imperfections and jerky motion of motors. Also, the links are not homogeneous as the CAD models due to the imperfections in 3-D printing. Due to these reasons, the limiting case for balance has gone down to 41.82° from 56° as observed in Figs. 11(a) and 8(a) respectively.

Figures 10(b), 10(d) and 11(b) shows the corresponding values of yaw and pitch from the feedback data from IMU for the experiments conducted above for 27.5°, 33.23° and 41.82° respectively. In first two cases, there is significant change in the pitch and a small change in yaw as well. The change in yaw angle can be explained by observing the trajectory given to the robot. As the robot moves its arm along with the abdomen as shown in Fig. 9, there is small moment acting in the vertical direction due to the arm movement. As a result there is a change in yaw angle. This is clearly reflected in the Figs. 10(b), 10(d).

The limiting case of stability at 41.82°can be also verified by its yaw and pitch plot in Fig. 11(b). There is an abrupt disturbance in Fig. 11(b) at time 10 s, which points towards the instability of the robot at the corresponding abdominal angle. Hence, the IMU data plays a crucial role in maintaining stability of the robot.

VI. CONCLUSIONS AND FUTURE WORK

This work presents the modifications to Poppy robot, for handling a task with more efficiency and power. Design of the robot was significantly modified to replace the original MX-28 servos with MX-64 having a greater torque range. The ankle joints and arms were modified and feet were redesigned in order to make robot more robust. A methodology for calculating ZMP using FSR was discussed. Simulations were carried out for finding limiting cases of balance for forward bending of the abdominal joints using ZMP. Using the FSRs, the ZMP of the real robot was calculated and the limiting cases of balancing were compared with the simulation results. The simulation and experimental results of ZMP are comparable in cases (case I and II) of small angular bending. But stability margins in simulation and real robot differs, which calls for using more precise inertia parameters of the real robot in the simulation. This will help to achieve much closer simulation results to the actual robot.

The immediate future work would be developing a more accurate representation of the robot for dynamic control of the robot. There are multiple future directions which can be explored using ZMP and IMU feedback, which includes walking on uneven terrain and lifting of heavy objects while maintaining balance. Also as a part of the future work, we plan to explore the controlling of articulated torso and the robot's 27 DOF in a USAR setting.

REFERENCES

[1] M. Hirose and K. Ogawa, "Honda humanoid robots development," *Philosophical Transactions of the Royal Society of London A: Mathematical, Physical and Engineering Sciences*, vol. 365, no. 1850, pp. 11–19, 2007.

[2] S. Kuindersma, R. Deits, M. Fallon, A. Valenzuela, H. Dai, F. Permenter, T. Koolen, P. Marion, and R. Tedrake, "Optimization-based locomotion planning, estimation, and control design for the atlas humanoid robot," *Autonomous Robots*, vol. 40, no. 3, pp. 429–455, 2016.

[3] C. L. Vaughan, "Theories of bipedal walking: an odyssey," *Journal of biomechanics*, vol. 36, no. 4, pp. 513–523, 2003.

[4] M. Vukobratović and J. Stepanenko, "On the stability of anthropomorphic systems," *Mathematical biosciences*, vol. 15, no. 1-2, pp. 1–37, 1972.

[5] M. Dekker, "Zero-moment point method for stable biped walking," *Eindhoven University of Technology*, 2009.

[6] N. Kanehira, T. Kawasaki, S. Ohta, T. Ismumi, T. Kawada, F. Kanehiro, S. Kajita, and K. Kaneko, "Design and experiments of advanced leg module (hrp-2l) for humanoid robot (hrp-2) development," in *Intelligent Robots and Systems, 2002. IEEE/RSJ International Conference on*, vol. 3. IEEE, 2002, pp. 2455–2460.

[7] https://www.tekscan.com/products-solutions/force-sensors/a201/, "Flexiforce a201 sensor," *Tekscan*, 2014.

[8] G. Metta, G. Sandini, D. Vernon, L. Natale, and F. Nori, "The icub humanoid robot: an open platform for research in embodied cognition," in *Proceedings of the 8th workshop on performance metrics for intelligent systems*. ACM, 2008, pp. 50–56.

[9] K. J. Muecke and D. W. Hong, "Darwins evolution: Development of a humanoid robot," in *2007 IEEE/RSJ International Conference on Intelligent Robots and Systems*. IEEE, 2007, pp. 2574–2575.

[10] S. Shamsuddin, L. I. Ismail, H. Yussof, N. I. Zahari, S. Bahari, H. Hashim, and A. Jaffar, "Humanoid robot nao: Review of control and motion exploration," in *Control System, Computing and Engineering (ICCSCE), 2011 IEEE International Conference on*. IEEE, 2011, pp. 511–516.

[11] M. Lapeyre, P. Rouanet, J. Grizou, S. Nguyen, F. Depraetre, A. Le Falher, and P.-Y. Oudeyer, "Poppy project: Open-source fabrication of 3d printed humanoid robot for science, education and art," in *Digital Intelligence 2014*, 2014, p. 6.

[12] Y. Ogura, H. Aikawa, K. Shimomura, H. Kondo, A. Morishima, H.-o. Lim, and A. Takanishi, "Development of a new humanoid robot wabian-2," in *Proceedings 2006 IEEE International Conference on Robotics and Automation, 2006. ICRA 2006.* IEEE, 2006, pp. 76–81.

[13] I. Mizuuchi, R. Tajima, T. Yoshikai, D. Sato, K. Nagashima, M. Inaba, Y. Kuniyoshi, and H. Inoue, "The design and control of the flexible spine of a fully tendon-driven humanoid" kenta"," in *Intelligent Robots and Systems, 2002. IEEE/RSJ International Conference on*, vol. 3. IEEE, 2002, pp. 2527–2532.

[14] A. Billard, B. Robins, J. Nadel, and K. Dautenhahn, "Building robota, a mini-humanoid robot for the rehabilitation of children with autism," *Assistive Technology*, vol. 19, no. 1, pp. 37–49, 2007.

[15] E. Guizzo and E. Ackerman, "The hard lessons of darpa's robotics challenge [news]," *IEEE Spectrum*, vol. 52, no. 8, pp. 11–13, 2015.

[16] O. Ly, M. Lapeyre, and P.-Y. Oudeyer, "Bio-inspired vertebral column, compliance and semi-passive dynamics in a lightweight robot," in *International Conference on Robots and Systems*, 2011.

[17] M. VACEK, J. ŽILKOVÁ, and M. PÁSTOR, "Regulation of dynamixel actuators in robot manipulator movement," *Acta Electrotechnica et Informatica*, vol. 14, no. 3, pp. 32–35, 2014.

[18] S. Kajita, H. Hirukawa, K. Harada, and K. Yokoi, *Introduction to humanoid robotics*. Springer, 2014, vol. 101.

[19] P. Sardain and G. Bessonnet, "Forces acting on a biped robot. center of pressure-zero moment point," *IEEE Transactions on Systems, Man, and Cybernetics - Part A: Systems and Humans*, vol. 34, no. 5, pp. 630–637, Sept 2004.

[20] D. A. Winter, "Human balance and posture control during standing and walking," *Gait & posture*, vol. 3, no. 4, pp. 193–214, 1995.

[21] F. Varesano, "Freeimu: An open hardware framework for orientation and motion sensing," *arXiv preprint arXiv:1303.4949*, 2013.